Basalt Mounds and Adjacent Depressions Attract Contrasting Biofacies on a Volcanically Active Middle Miocene Coastline (Porto Santo, Madeira Archipelago, Portugal)

Ana Santos[1*], Eduardo Mayoral[1], Markes E. Johnson[2], B. Gudveig Baarli[2], Carlos M. da Silva[3], Mário Cachão[3], Jorge Ledesma-Vázquez[4]

[1.]Departamento de Geodinámica y Paleontología, Facultad de Ciencias Experimentales, Campus de El Carmen, Universidad de Huelva, Avda. 3 de Marzo, s/n, 21071 Huelva, Spain

[2.]Department of Geosciences, Williams College, Williamstown, MA 01267 USA

[3.]Departamento de Geologia and Centro de Geologia, Faculdade de Ciências, Universidade de Lisboa, Campo Grande, 1749-016 Lisbon, Portugal

[4.]Facultad de Ciencias Marinas, Universidad Autónoma de Baja California, Ensenada, BC 22800, Mexico

* Corresponding author. (AS) asantos@dgyp.uhu.es

Abstract

Small basalt mounds with encrusting corals and inter-mound carbonate sandy zones with abundant rhodoliths corresponding to an ancient intertidal to shallow-water sea floor are exhumed from overlying volcaniclastic deposits and basalt lava flows at Pedra de Água on Ilhéu de Cima off Porto Santo, one of the islands of the northeastern Atlantic Madeira Archipelago (Portugal). The mounds rise above the surrounding surface to attain a height of about half a meter. The mounds exhibit an *in situ* assemblage of hermatypic corals, dominated by *Tarbellastrae* and *Solenastrea*. They formed as massive (4.2 × 1.9 m

average length), isolated patches in a protected bay close to shore eroded from an uneven basalt substrate dated to the Middle Miocene (14 to 15 Ma). The slightly deeper zones between basalt mounds, which alternate with them over a distance of more than 20 m, are covered mainly by coarse carbonate sand on which rhodoliths up to 14.8 cm in diameter are preserved *in situ*. Many rhodoliths have grown around a basalt core, which indicates a local, nearshore source for development. Complete burial of the elevated coral settlements and intervening low zones populated by rhodoliths occurred when volcanic lapilli and other tephra catastrophically buried this part of the rocky shore. The rhodoliths and coral assemblages exposed in an area of 12 m^2 were canvassed systematically using census quadrats to quantify community relationships.

Key words rocky shores, Miocene, shallow-subtidal zonation, corals, rhodoliths, Obrution deposits, Volcanic island

Introduction

Rocky shores constitute a special environment with an evolutionary history of a dynamic ecosystem since the Precambrian (Johnson and Baarli 2012). Geographically they ranged across tropical to boreal latitudes, just as today (Johnson 2006). In this context, hard stable substrates exposed to intertidal and shallow-subtidal waters provide exceptional conditions for colonization by boring and encrusting organisms. The *in situ* fossils of these organisms, mostly algae and invertebrates, represent potential tools in paleoenvironmental analysis of shoreline settings. Not all unconformities, however, are

equally significant as ancient coastlines (Johnson 1988). Typically, those rocks most resistant to coastal erosion, such as basalt or quartzite, tend to form unconformity surfaces with appreciable topographic relief under transgressive conditions that promote the development of intertidal boulder beds and cliffs.

Nearly all studied former islands are situated on epicontinental platforms or continental shelf margins (e.g., Lescinsky et al. 1991; Doyle et al. 1997; Johnson et al. 1988, 1995, 2010; Johnson and Ledesma-Vázquez 1999; Betzler et al. 2000; Wilson and Taylor 2001; Surlyk and Sørensen 2010). Despite widespread availability for study short-term biological colonization on rockgrounds (see Taylor and Wilson 2003), the paleo coasts of oceanic islands are surprisingly under-represented. In fact, few observations are recorded on the dynamics between coastal sedimentation and settlement patterns in the intertidal to shallow subtidal zone with respect to intermittent volcanism and related tectonics (Meco et al. 2007; Johnson et al. 2010).

The present contribution is the fourth in a series of studies on the paleoecology of Miocene shallow-water marine benthic communities on basaltic rocky shores of Ilhéu de Cima (Madeira Archipelago, Portugal). Santos et al. (2011) focused on a Miocene rocky-shore biota from Ilhéu de Cima, providing a clear example of fossil marine invertebrates preserved on a wave-cut platform and related cliff face of solid basalt. Johnson et al. (2011) described an extraordinary deposit of fossil rhodoliths washed against a Miocene rocky shore as a result of storms of near-hurricane strength, and Santos et al. (2012a) re-evaluated the extent of organic boring on basalt surfaces on the same islet.

This paper describes two adjoining Miocene biofacies reflecting a definite pattern of intertidal to shallow-water zonation preserved on a low–relief rocky shore at a place

named Pedra de Água (Fig.1). At this locality, encrusting corals were briefly established on low basalt mounds and surrounded by a coarse carbonate sandy gravel substrate that supported many rhodoliths prior to sudden burial by volcanic lapilli and other tephra, thereafter succeeded by massive basaltic flows. Obrution deposits similar to this are otherwise well known in the paleoecological literature (Brett et al. 1997), but rare in terms of sudden burial by volcaniclastic material. Experience with Holocene and modern settings where local extermination of coral communities took place should, however, facilitate our search for comparable patterns in the geologic record (Heikoop et al. 1996; Pandolfi et al. 2006). Here, we investigate the dynamics between environmental conditions and biotic colonization from a Miocene sheltered cove on Pedra de Água that became catastrophically entombed by volcaniclastic material.

Location and geological setting

Portugal's Madeira Archipelago sits 650 km off the shores of Moroccan Africa in the North Atlantic Ocean. Porto Santo is an outlying island located 50 km northeast of the principal island of Madeira (Fig. 1). Ferreira (1997) produced a geological map of Porto Santo, including its various satellite islets. The second largest is Ilhéu de Cima with a perimeter of approximately 3 km and maximum elevation of 115 m. Fossiliferous sedimentary successions occur in several places on the main island of Porto Santo in relation to the transition between two major volcanic units: a lower trachytic to basaltic submarine basal volcanic complex with ages ranging from 18.8 to 13.5 Ma; and an upper subaerial alkali basaltic to hawaiitic complex dated between 14 and 10.2 Ma (Ferreira 1985). Based on calcareous nannofossil assemblages at Lombinhos on the east side of

Porto Santo, Cachão et al. (1998) correlated sedimentary units to the Middle Miocene, lower Serravalian (Calcareous Nanofossil biozone CN4 of Okada and Bukry 1980). A comparable age of about 14 to 15 Ma is extrapolated for sedimentary intercalations between volcanic rocks on Ilhéu de Cima.

The study site described in this paper is located approximately 225 m northwest of the only landing place on Ilhéu de Cima, at an elevation of 7 m above mean sea level (Fig. 1).

Methods

Two methods were used to test the visual impression at the outcrop scale of physical and biological zonation preserved intact on the rocky paleo-shore at Pedra de Água. The first, was the establishment of transect lines with grids, for methodical sampling of the Middle Miocene encrusting corals and associated rhodolith beds (Fig. 2). Four transects 0.5 m apart (labeled A-D) were laid out parallel to the base of the present-day cliff line across the fossil deposit located approximately 30 m inland from the present shore. A grid (0.5×0.5 m in size and divided into twenty-five units of 10 × 10 cm each) was deployed and moved along each transect line to collect data on fossil content and to map settlement patterns. The same operation was applied to low-lying areas between the basalt mounds, where rhodoliths are commonly found on a thin bed of coarse bioclastic debris. The number of grid samples recorded for each transect line was 24. The completed survey entailed full coverage of an area 12 by 2 m (24 m^2). All fossil biogenic components within this area were identified to species level where possible and tabulated to graphically show how populations in each category change grid-by-grid along each of the

transects (A to D). Bioerosional structures were also identified when present. Criteria used to distinguish *in situ* material from reworked material included: (1) orientation of corallites, (2) whether or not fossil bivalves are articulated, and (3) presence or absence of encrusting coralline algae. Coral identification conforms to the taxonomy followed by Best and Boekschoten (1982) in their revision of Chevalier (1972).

In order to facilitate the sample analyses and map transitional boundaries between the two biofacies, three blocks (16 grids to one block, equal to 4 m^2) were chosen for illustration from the full array (Fig. 2). The blocks are labeled 1 (outside of the cliff line to the NW), 2 (middle block) and 3 (outside of the cliff line to the SE). Every fossil and every area with bare substrate was plotted precisely in place.

A second supplementary method of data collection was applied randomly on the outcrop surface with the purpose of collecting data on size variation in rhodoliths and the extent to which rhodoliths formed around basalt cores. The study on size variation and nucleation of 100 rhodoliths was simplified by determining only the two major visible axes of their shape and rock core. In addition, 39 isolated rhodoliths were measured along the three axes – long (L), intermediate (I), and short (S) – in order to plot them on the Sneed and Folk (1958) pebble-shape diagram to generate the sphericity index for rhodoliths after Bosence (1976, 1983a). Thin-sections were made of selected rhodoliths so that their inner arrangements could be described and the constituent coralline algae identified.

Stratigraphic sucession

An irregular subaerial basaltic flow (with large columnar disjunctions) provided the substrate for the fossiliferous horizon at Pedra de Água, which accumulated as a rhodolith biocalcarenite over the lowermost depressions (near the current seashore), changing eastward to fossiliferous limestone with rhodoliths on a more level surface (Fig. 3). Here, near the present day cliff line about 30 m inland, the uppermost sediment-free basaltic substrate is almost completely covered by *in situ* encrusting corals. In turn, these fossiliferous deposits are covered by approximately 1.5 m of yellow-orange volcanic tuff with an irregular thickness, followed immediately above by a 1 m thick volcanic breccia. The succession continues with a 13 m thick basaltic lava flow. Above this volcanic unit is another whitish fossiliferous horizon, mainly composed of corals. The succession is completed by two to three subaerial basalt flows separated by a single marker bed of red tuff (Fig. 3).

The lowermost volcanic unit irregularly thickens towards the northwest, forming a rocky ramp at Furninha, against which the lower fossiliferous unit ends (Fig. 1). The lava flow above the fossiliferous unit also thickens northward, while the subsequent subaerial basaltic surfaces have an overall sigmoid shape with maximum thickness attained towards the southeastern end of the island. The upper units formed under subaerial conditions may be slightly younger in age relative to the fossiliferous units interbedded with submarine hyaloclastites dated at 15-14 Ma (Cachão et al. 1998) located some 5 km northeast, at Lombinhos (on the adjacent main island of Porto Santo).

Paleontological analysis

Census Data

The transects from A to D (Fig. 2) show no significant changes from the present cliff line in the present-day seaward direction. However, the frequency data on a grid-by-grid basis for each fossil entity revealed two distinct biofacies along the paleoshore (Fig. 4a-b). There is a distinct spatial affinity between the locations of the corals and *Gastrochaenolites* borings, while the rhodoliths cluster separately (Figs. 4a, 5a-b).

The results of the systematic survey across the surface of the paleoshore are plotted as "ecologic zonation" maps representing half of the total surface area studied (blocks 1, 2 and 3; Fig. 6a-c). As summarized in Table 1, 50% of the mapped area (12 m^2) was occupied by bioclastic coarse and unsorted sandy gravel and in 7% the gravel was mixed with rhodoliths. The rest of the exposed surface was bare basalt (27%) and corals attached directly on it (16%). An unknown proportion of bare basalt in the census area may have been stripped of its carbonate crust and/or other distinguishable macrofossils as a result of Recent erosion, but the spatial distribution of the remaining fossils still reveals a distinct pattern. A thick white carbonate rind is recognized in some places on top of the basalt.

If we focus on the distribution of substrate nature and *in situ* fossils by individual blocks (Table 1), block 1 and 2 are those with the highest percentage of coarse and unsorted sandy gravel mixed with rhodoliths (63% and 61%, respectively). Block 3 exhibits only 46% of coarse and unsorted sandy gravel mixed with rhodoliths. The number of rhodoliths counted is 47 both for blocks 1 and 2, but rhodoliths are more abundant in block 3 with 74 individuals (Table 1). The number of rhodoliths per square-meter of sand is 18.7 for block A, 19.3 for block B and 40.2 for block C. In contrast, the percentage of bare basalt surface is greater (39%) for block 3, but only 28% and 15% for

blocks 2 and 1, respectively. Regarding corals, block 1 presents the highest percentage of surface occupied by encrusting corals (22%), followed by block 3 with 15% and block 2 with only 11%. Block 2 contains the largest number of *Spondylus* sp. (six individuals). Both of the other two blocks contain only two individuals each.

Although abundance is high, fossil diversity on the Pedra da Água rocky shore is quite low. Only two coeval benthic communities are represented: a mound community (zone of coral encrustation) and an inter-mound community (zone of rhodolith pavement).

Mound community (zone of coral encrustation)

An assemblage of encrusting colonial corals dominates the tops of the basalt mounds, corresponding to the higher local topography and the more exposed rocky intertidal to shallow-subtidal environment. The mounds are circular in shape (maximum length: 8.5 × 3 m; minimum length: 2 × 1 m), and rise above the surrounding soft bottom for about half a meter.

At least two species of scleractinian corals (*Tarbellastrea reussiana* Milne-Edwards and Haime, 1850 and *Solenastrea* sp.) are present in the mound community. Figure 7 a illustrates the closely packed coral colonies attached directly to the basalt surface and preserved in growth position. Lesser elements such as the epifaunal bivalve *Spondylus* sp., the encrusting bryozoan *Conopeum* sp., and the coral-inhabiting barnacle *Ceratoconcha costata* Kramberger-Gorjanović (1889) are also present. Representative trace fossils present in the corals include borings produced by demosponges (*Entobia* isp.), coral-inhabiting barnacles (*Imbutichnus costatum* Santos et al., 2012) and borings of

bivalves (*Gastrochaenolites torpedo* Kelly and Bromley, 1984) (Fig. 7 b). *Imbutichnus costatum* structures are found exclusively on *Tarbellastrea* sp. indicating a clear host preference by the producer *Ceratoconcha costata* (Santos et al. 2012b). The post-mortem bivalve borings are arranged perpendicularly to the coral surface and most of them are truncated, presenting an average diameter of 1.5 cm. Counts from the sampling grid yielded an average of ten *T. reussiana*/*Solenastrea* sp. colonies/m^2. The average number of *G. torpedo* /block was 201/m^2 for block 1, 57/m^2 for block 2, and 65/m^2 for block 3 (Table 1).

Spondylus sp. with articulated valves occurs preserved in life position among the corals. Some of the shells are partially covered with crustose coralline algae and encrusting bryozoans. As noted previously, it is possible to recognize in some places on top of the basalt a thick conspicuous white carbonate rind. Such crusts are devoid of fossils. Both rhodoliths and bioturbation structures are absent. For a more generalized paleoecologic setting of the described biofacies see Table 2.

Inter-mound community (zone of rhodolith pavement)

The inter-mound community consists entirely of rhodoliths often encrusted by serpulids and showing *Gastrochaenolites* isp. bioerosion. Lumpy in morphology, clustered rhodoliths are restricted to a separate zone occupying a lower topographic position between the raised patches of basalt. Composed of crustose coralline red algae, these rhodoliths are mainly multispecific. *Lithophyllum* and *Sporolithon* most commonly occur together (Fig.8a), although monospecific rhodoliths of *Sporolithon* sp. have also been identified, as well as a less common combination of *Lithophyllum* and *Hydrolithon* (Fig.

8b). The matrix in which the rhodoliths occur contains very coarse and unsorted sandy gravel (average diameter 2 mm) with clasts up to 10 mm in diameter, as well as some shell fragments derived from *Spondylus* sp. (Fig. 9a). The packing density of rhodoliths varies from 18.7/m^2 and 19.3/m^2 for block 1 and 2, respectively, to 40.2/m^2 for block 3.

The shape of these rhodoliths is spheroidal to ellipsoidal (according to Bosence's (1983b) growth terminology (Fig. 10). The diameter of the rhodoliths varies from a minimum of 1.9 cm to a maximum of 14.8 cm. Most of the rhodoliths include a nucleus composed of rock (Fig. 9b). The high correlation coefficient (R^2= 0.82) between data for maximum diameters of rhodoliths and cores indicates a positive, linear relationship (Fig. 11) showing that the rock nucleus influenced the general shape of the rhodolith. The size of rock cores tends to very large (4.7 cm on average) compared to the total size of the rhodoliths with an average size of 6.4 cm (Fig. 9b). The average thickness of the coralline red algae crust is thus less than 1.7 cm with little difference between small and large rhodoliths.

In thin-section, rhodoliths reveal a massive inner arrangement with no macroscopic cavities. The inner arrangement is laminar-concentric around the nucleus to slightly columnar towards the surface according to Bosence's (1983b) nomenclature. Thin-sections show some degree of reworking and erosion, although many rhodoliths are unabraded. Rare instances of two basalt cores or cores consisting of corals also are found. Cross-sections through rhodoliths do not show a faunal succession nor overgrowth patterns.

No bioturbation structures are recognized in the matrix in which the rhodoliths occur. For a more generalized paleoecologic setting of the biofacies see Table 2.

Discussion

Water depth

As evaluated by some authors (James and MacIntyre 1985; Bourillot et al. 2009), paleotopography is the essential controlling factor for coral-reef location because reefs flourish in elevated zones exposed to good marine circulation. Also, light conditions as well as the ambient water energy influence the growth form of individuals that compose the coral assemblages (Mankiewicz 1995).

According to Bourillot et al. (2009), coral communities that are dominated by domal forms, such as *Tarbellastrea*, indicate shallow, high-energy waters. Another argument in support for this interpretation derives from the presence of abundant bivalve borings on the coral colonies of Pedra de Água, generally suggesting a very shallow marine environment (waters only a few meters deep) with a low or zero sedimentation rate (Bromley and Asgaard 1993; Bromley 1994). The size of pebbles and cobbles which the rhodoliths encrusted suggests a source area close to the paleoshore at Pedra de Água, as does the immediately overlying tuff layer. Thus, the water depth in this area was shallow and well above the fair-weather wave-base.

Coralline red algal taxa forming rhodoliths have often been used to infer paleodepth. However, Rasser and Piller (1997) showed that depth analysis based on genera was problematic. Such analyses are best done at species level. The genus *Sporolithon* is generally most abundant below 20 m in the northern hemisphere and in tropical areas (Adey et al. 1982; Perrin et al. 1995; Aguirre et al. 2000; Braga and Bassi 2007; Basso et al. 2009). However, there are exceptions to this. Basso et al. (2009)

described Recent rhodoliths formed by *Sporolithon* from intertidal pools and tidal channels on wave-cut platforms from New Zealand, while Baarli et al. (2012) recorded rhodoliths formed by the same algae in Quaternary calcareous sands deposited in water depths of less than 6.5 m in Baja California (Mexico).

Substrate

The studied corals at Pedra de Água are directly cemented to mounds of basalt, which is in accordance with their environmental preferences because these encrusting coral colonies developed preferentially on hard rather than soft substrates (Cabioch et al. 1995). According to Johnson and McKerrow (1995), very few examples are known of fossil corals attached directly to inorganic surfaces. They documented encrustation of the Early Jurassic coral *Heterastrea* sp. on Carboniferous limestone at Southerndown (South Wales). Johnson and Baarli (1987) recorded *Favosites* sp. from the Upper Ordovician of Hudson Bay encrusting quartzite boulders in a rocky-shore setting. An unidentified scleractinian coral has been shown by Lescinsky et al. (1991) to encrust andesite boulders in a rocky-shore setting of Late Cretaceous age in Baja California (Mexico). The colonial corals *Tarbellastraea reussiana* (Milne-Edwards and Haime, 1850) and *Isophyllastrea orbignyana* (Mayer, 1864) were reported encrusting basaltic substrate in a rocky-shore setting of Middle Miocene age in Ilhéu de Cima (Madeira Archipelago; Santos et al. 2011).

Water energy

298 The fossil encrusting corals occurring on the top of the basalt mounds at Pedra de Água
299 were not originally covered by the sediment that presently fills the surfaces around them
300 prior to burial by tuff. It is clearly seen in the base of the cliff that the overlying volcanic
301 tuff bed (Figs. 3, 12) formed directly on the top of the corals and the rhodoliths alike,
302 estending across both ecological zones, that was responsible for their demise. Therefore,
303 the wave energy at Pedra de Água locality was sufficient to prevent sediment grains from
304 settling to suffocate corals and also to carry smaller eroded basalt clasts seaward, but
305 insufficient to do much damage to the coral colonies because they were firmly attached in
306 a higher topographic position. The eroded basalt clasts filled the lower areas of
307 paleorelief around the coral mounds on the basalt substrate and were readily adopted as
308 nuclei by the coralline red algae living there. The presence of rhodoliths also implies a
309 low sedimentation rate and unlithified substrate (Bosence 1991) subjected to turbulent
310 waters (Adey and Burke 1976; Johnson et al. 2009).

311 Rhodoliths have an unattached mode of life. Marrak (1999) suggested that high
312 disturbance by infaunal organisms could be an important agent to stimulate overturning.
313 However, considering the lack of bioturbation, the large, heavy rhodoliths, and the
314 associated thin, coarse sediment layer at Pedra de Água, wave energy was the more likely
315 responsible for rhodolith overturning.

316 The external morphology and internal structure of rhodoliths may be useful
317 indicators of hydraulic energy. Spheroidal to ellipsoidal shape, massive inner
318 arrangement with a uniform lumpy surface growth-form and the occurrence of a lithic
319 nucleus are consistent with a frequent and regular overturning of the rhodoliths by wave
320 action (e.g., Bosellini and Ginsburg 1971; Bosence 1983a, b; Scoffin et al. 1985; Johnson

and Hayes 1993; Steller and Foster 1995; Foster et al. 1997; Gischler and Pisera 1999; Bassi et al. 2009). Thin-sections also show a symmetrical accretion around the core and few empty voids, both of which indicate high water energy and frequent overturning (Bassi et al. 2009). Likewise, the low presence of sediment in the interior of the rhodoliths is often considered to be evidence of a low sedimentation rate or of a regular overturning of the rhodoliths on the sea floor (Basso 1998).

There is some evidence of abrasion of the Pedra de Água rhodoliths, as is often the case for rhodoliths in fairly shallow waters on a coarse bioclastic substrate (Bassi et al. 2009). Dead rhodoliths may be exploited as substrate for new colonization leading to polyspecific rhodoliths (Basso et al. 2009), which are commonly encountered in this study.

Basso (1998) demonstrated that the packing is crucial in explaining the hydraulic behavior of rhodoliths. With a higher density, stronger wave action is needed to move the rhodoliths. Comparing rhodoliths at Pedra de Água on the southwest side of Ilhéu de Cima with rhodoliths at Cabeço das Laranjas on the northeast side of the islet (Johnson et al. 2011), some 300 m away, they are of comparable sizes, but the thickness of the deposits and their packing density differs profoundly. The former site displays less than 40 rhodoliths per square meter while the latter shows more than 200 /m^2. The rhodolith assemblage at Cabeço das Laranjas was identified as transported into the site from deeper off-shore banks by hurricanes or strong storms. In contrast, the rhodoliths at Pedra de Água formed a living community with a density level and bed thickness sufficiently limited to promote rotation leading to even growth around a rock core.

Rhodolith nucleus

The shape of pebbles and cobbles present in the sediment matrix was responsible for the ultimate shape of the rhodoliths (Lund et al. 2000). This is in accordance with the data obtained by Scoffin et al. (1985) from Recent shallow reef rhodoliths at Cook Islands (central Pacific). These authors analyzed and compared different rhodolith nuclei (basalt pebbles, stick corals, mussel valves, and gastropods) with the final shape of the algae and concluded that most of these rhodoliths, at least initially, are greatly influenced by the shape of its nucleus. As a general rule, the more spherical the nuclei (e.g., basalt pebbles) the more regular the concentric encrustations, while on tabular or bowl-shaped nuclei (e.g., mussel shells) the encrustations are of uneven thickness (Scoffin et al. 1985).

Another good example is the Pliocene rhodolith deposits at Punta San Francisquito in the Gulf of California studied by Johnson et al. (2009), because there relatively large rhodoliths have a solid granodiorite core. At present, this Pliocene site is the only known locality in the Gulf of California where this peculiarity is known to occur. However, some differences exist between the two places in terms of overall rhodolith size. The rhodoliths from Punta San Francisquito measure 5 cm across on average with calcareous rinds that completely enclose granodiorite pebbles up to 3 cm in diameter (Johnson et al. 2009). This is in contrast to the much larger Miocene rhodoliths at Pedra de Água. Johnson and Hayes (1993) studied small andesite pebbles from the Late Cretaceous at Las Minas (Pacific coast of northern Baja California), with rinds 5 mm to 8 mm in thickness. This effectively doubled the diameter of the pebbles as a consequence of algal encrustation. In this particular case, the relative proportion of the crust was larger than at Pedra de Água, but the size and shape of the nuclei still primarily influenced the

shapes of nucleated rhodoliths as found in many other studies (Basso and Tomaselli 1994; Ballantine et al. 2000; Bassi et al. 2009).

Generally, the Pedra de Água rhodoliths have a uniform size and shape and a basalt core with a thin crust of algae of about the same thickness regardless of size. This suggests there was just one population with the same, relatively short history of development, which could only be achieved by fairly frequent movement.

Paleoenvironmental interpretation

According to the surrounding topography at Pedra de Água (Fig. 1), the study area features encrusting corals on basalt mounds that grew within a small protected embayment at the paleo-island at Ilhéu de Cima. Wave action within the bay was still sufficient to promote the growth of small patches of corals and to keep the rhodoliths in between the basalt mounds in motion. The fact that some rhodoliths display signs of erosion and the coarse bioclastic matrix suggest some degree of bottom reworking by currents as shown by Bassi (1998). In this context, the topographic configuration may have controlled local current patterns. The patches of corals on low mounds of basalt are surrounded by sandy gravel and rhodolith beds. Wave action from the south or southwest was the only possible source for wind-driven waves to reach the shelf at this locality. This is confirmed by Santos et al. (2011), who show that the Miocene coastline ran paralell to the present one southeast of Pedra de Água. This is in marked contrast to Cabeço das Laranjas on the opposite side of the islet, where much sediment was transported from offshore banks by strong storms or hurricanes from the southeast or east and piled up against paleocliffs and boulders (Johnson et al. 2011).

The *in situ* preservation of corals and rhodoliths is a result of the rapid, catastrophic burial of the small embayment at Pedra de Água by a layer consisting of volcanic lapilli and finer tephra (Fig. 12). As such, the Miocene fossil assemblages representing two different biofacies at this locality are interpreted as obrution deposits according to the criteria set out by Brett et al. (1997). The rapid burial of coral beds at present and in the geologic past is a well-documented phenomenon (e.g., Heikoop et al. 1996; Pandolfi et al. 2006; Multer 2006; Reuter and Piller 2011). This is the first well documented example of obrution deposits due to volcanic ejecta from the Miocene. Essentially, the biofacies preserved intact at Pedra de Água constitute a kind of paleontological Pompeii for Miocene coastal habitats.

The Middle Miocene fossil assemblages at the Pedra de Água site do not signify a genuine rocky shore, but may be seen as a *in situ* preserved rocky shore communities because, in agreement with Lescinsky et al. (1991), they represent a near-shore, hard-substrate community influenced by wave energy.

Conclusions

(1) Two zones with distinctly different biotic communities developed in adjacent, shallow subtidal areas: (a) a zone of coral encrustation and (b) a zone of rhodolith pavement. The first zone is characterized by encrusting colonial dome-shaped scleractinian corals accompanied by subordinate components such as the cemented bivalve *Spondylus*, boring bivalves producing *Gastrochaenolites* bioerosional structures, and bryozoans. The second zone is characterized by the

presence of rhodoliths with a lumpy morphology that accrued as free rolling algal nodules.

(2) These zones occupied two distinct but interpenetrating high energy shallow subtidal areas corresponding to the same surface of that former stretch of the coast: (a) basalt mounds forming hard substrates occupying topographic highs and (b) about a half meter deeper, a soft sandy gravel bottom occupying topographic lows between the basalt mounds.

(3) Based in part on the depositional style of the rhodolith beds the southwestern side of Miocene Ilhéu de Cima represents a comparatively sheltered setting in contrast to the storm-impacted northeastern side of the islet.

(4) The Pedra de Água outcrop features the first well documented example of obrution deposits affecting two coeval *in-situ* preserved Miocene paleocommunities, a coral-dominated and a rhodolith-dominated paleocommunity, which were catastrophically buried by volcanic lapilli and fine tephra.

Acknowledgments

A. Santos received financial support from the Ministry of Science and Technology of Spain in the form of a Juan de la Cierva contract (Refª JCI-2008-2431). Johnson's participation was supported by a travel grant from the Class of 1945 Faculty World Fellowship during sabbatical leave from Williams College in 2009–2010. Participation by Ledesma-Vázquez was supported by travel grants from the Universidad Autónoma de

Baja California under the 14th Research Program, and from the Cuerpo Académico de Geología Costera/Programa Integral de Fortalecimiento Institucional. Financial support was also given by the Junta de Andalucía (Spanish government) to the Research Group RNM316 (Tectonics and Palaeontology) and by the Spanish DGI Project CGL 2010-15372/BTE. The Portuguese Navy and Porto Santo Municipality (Porto Santo Verde) provided transportation to and from Ilhéu de Cima. Rafael Riosmena-Rodríguez (Universidad Autónoma de Baja California Sur, La Paz, Mexico) kindly provided the generic identifications for the Pedra de Água rhodoliths. Finally, the authors are grateful to Franz Fürsich (Facies Editor-in-Chief), Davide Bassi (University of Ferrara, Italy), and Eberhard Gischler (University of Frankfurt, Germany) for helpful and constructive comments, which significantly improved the manuscript.

References

Adey WH, Burke R (1976) Holocene bioherms (algal ridges and bank-barrier reefs) of the eastern Caribbean. Geol Soc America Bull 87:95–109

Adey WH, Townsend RA, Boykins WT (1982) The crustose coralline algae (Rhodophyta: Corallinacea) of the Hawaiian Islands. Smithson Contrib Mar Sci 15:1–74

Aguirre J, Riding R, Braga JC (2000) Late Cretaceous incident light reduction evidence from benthic algae. Lethaia 33:205–213

Baarli BG, Santos A, Silva CM da, Ledesma-Vázquez J, Moyoral E, Cachão M, Johnson ME (2012) Diverse macroids and rhodoliths from the Upper Pleistocene of Baja Califórnia Sur, México. J Coast Res 28:296–305

Ballantine DL, Bowden-Kerby A, Aponte NE (2000). *Cruoriella* rhodoliths from shallow-water back reef environments in La Parguera, Puerto Rico (Caribbean sea). Coral Reefs 19:75–81

461 Bassi D (1998) Coralline algal facies and their palaeoenvironments in the Late Eocene of
462 Northern Italy (Calcare di Nago, Trento). Facies 39:179–202
463 Bassi D, Nebelsick JH, Checconi A, Hohenegger J, Iryu Y (2009) Present-day and fossil
464 rhodolith pavements compared: their potential for analysing shallow-water
465 carbonate deposits. Sediment Geol 214:74–84
466 Basso D (1998) Deep rhodolith distribution in the Pontian Islands, Italy: A model for the
467 paleoecology of a temperate sea. Palaeogeogr Palaeoclimatol Palaeoecol
468 137:173–187
469 Basso D, Nalin R, Nelson CS (2009) Shallow-water *Sporolithon* rhodoliths from North
470 Island (New Zealand). Palaios 24:92–103
471 Basso D, Tomaselli V (1994) Palaeoecological potentiality of rhodoliths: a Mediterranean
472 case history. In: Matteucci R, Carboni MG, Pignatti JS (eds) Studies on ecology
473 and paleoecology of benthic communities. Boll Soc Paleont Ital Spec Vol 2:17–27
474 Best MW, Boekschoten GJ (1982) On the coral fauna in the Miocene reef at Baixo, Porto
475 Santo (Eastern Atlantic). Netherlands J Zool 32:412–418
476 Betzler C, Martin JM, Braga JC (2000) Non-tropical carbonates related to rocky
477 submarine cliffs (Miocene, Almeria, southern Spain). Sediment Geol 131:51–65
478 Bosence DWJ (1976) Ecologic studies on two unattached coralline algae from western
479 Ireland. Palaeontology 19:71–88
480 Bosence DWJ (1983a) The occurrence and ecology of Recent rhodoliths – A review. In:
481 Peryt TM (ed) Coated grains. Springer-Verlag, Berlin, pp 225–242
482 Bosence DWJ (1983b) Description and classification of rhodoliths (rhodoids, rhodolites).
483 In: Peryt TM (ed) Coated grains. Springer-Verlag, Berlin, pp 217–224

484 Bosence DWJ (1991) Coralline algae: mineralization, taxonomy and palaeoecology. In:
485 Riding R (ed) Calcareous algae and stromatolites. Spinger-Verlag, Berlin, pp
486 98−113
487 Bosellini A, Ginsburg RN (1971) Form and internal structure of Recent algal nodules
488 (rhodolites) from Bermuda. J Geol 79:669–682
489 Bourillot R, Vennin E, Kolodka C, Rouchy J-M, Caruso A, Durlet C, Chaix C,
490 Rommevaux V (2009) The role of topography and erosion in the development and
491 architecture of shallow-water coral bioherms (Tortonian-Messinian, Cabo de
492 Gata, SE Spain). Palaeogeogr Palaeoclimatol Palaeoecol 281:92−114
493 Braga JC, Bassi D (2007) Neogene history of *Sporolithon* Heydrich (Corallines,
494 Rhodophyta) in the Mediterranean region. Palaeogeogr Palaeoclimatol Palaeoecol
495 243:189−203
496 Brett CE, Baird GC, Speyer SE (1997) Fossil lagerstätten: Stratigraphic record of
497 paleontological and taphonomic events. In: Brett CE, Baird C (eds) Paleontological
498 events – Stratigraphic, ecological, and evolutionary implications. Columbia
499 University Press, New York, pp 3−40
500 Bromley RG (1994) The palaeoecology of bioerosion. In: Donovan SK (ed) The
501 palaeobiology of trace fossils. Wiley, New York, pp 134−154
502 Bromley RG, Asgaard U (1993) Endolithic community replacement on a Pliocene rocky
503 coast. Ichnos 2:93−116
504 Cabioch G, Montaggioni LF, Faure G (1995) Holocene initiation and development of
505 New Caledonian fringing reefs, SW Pacific. Coral Reefs 14:131−140

506 Cachão M, Rodrigues D, Silva CM da, Mata J (1998) Biostratigrafia (nanofósseis
507 calcários) e interpretação paleoambiental do Neogénico de Porto Santo (Madeira),
508 (dados preliminares). Com Inst Geol Min 84:A185−A188
509 Chevalier J-P (1972) Les Scléractiniaires du Miocéne de Porto Santo (Archipel de
510 Madére. Annls Paléont Invert 58:141−164
511 Doyle P, Mather AE, Bennet MR, Bussel MA (1997) Miocene barnacle assemblages
512 from southern Spain and their palaeoenvironmental significance. Lethaia
513 29:267−274
514 Ferreira MP (1985) Evolução geocronológica e paleomagnética das ilhas do arquipélago
515 da Madeira - uma síntese. Mem Not Mus Lab Miner Geol Univ Coimbra
516 99:213−218
517 Ferreira MP (1997) Carta Geológica de Portugal, Folha da Ilha de Porto Santo. Ministério
518 da Economia, Escala 1:25,000. Instituto Geológico e Mineiro, Portugal.
519 Foster MS, Riosmena-Rogríguez R, Steller DL, Woelkerling WJ (1997) Living rhodolith
520 beds in the Gulf of California and their implications for paleoenvironmental
521 interpretation. In: Johnson ME, Ledesma-Vázquez J (eds) Pliocene carbonates and
522 related facies flanking the Gulf of California, Baja Califórnia, México. Geol Soc
523 Am, Speci Pap 318:127−139
524 Gischler E, Pisera A (1999) Shallow water rhodoliths from Belize reefs. N Jb Geol
525 Paläont Abh 214:71−93
526 Heikoop JM, Tsuijita CJ, Heikoop CE, Risk MJ, Dickin AP (1996) Effects of volcanic

ashfall recorded in ancient marine benthic communities: comparison of a nearshore and an offshore enviroment. Lethaia 29:125–140

James NP, MacIntyre IG (1985) Carbonate depositional environments. Part 1: Reefs. Colorado School Mines Quart 80:1–70

Johnson ME (1988) Why are ancient rocky shores so uncommon?. J Geol 96:469–480

Johnson ME (2006) Uniformitarianism as a guide to rocky-shore ecosystems in the geological record. Can J Earth Sci 43:1119–1147

Johnson ME, Baarli BG (1987) Encrusting corals on a latest Ordovician to earliest Silurian rocky shore, southwest Hudson Bay, Manitoba, Canada. Geobios 15:15–17

Johnson ME, Baarli BG (2012) Development of intertidal biotas through Phanerozoic time. In: Talent JA (ed) Earth and life: Global biodiversity, Extinction intervals and biogeographic perturbations through time. International Year of Planet Earth. Springer-Verlag, Dordrecht, The Netherlands. DOI: 10.1007/978-481-3428-1_5

Johnson ME, Baarli BG, Scott JH Jr (1995) Colonization and reef growth on a Late Pleistocene rocky shore and abrasion platform in western Australia. Lethaia 28:85–98

Johnson ME, Backus DH, Riosmena-Rodríguez R (2009) Contribution of rhodoliths to the generation of Pliocene-Pleistocene limestone in the Gulf of California. In: Johnson ME, Ledesma-Vázquez J (eds) Atlas of coastal ecosystems in the western Gulf of California: tracking limestone deposits on the margin of a young sea. The University of Arizona Press, Tucson, pp 83–94

549 Johnson ME, Hayes ML (1993) Dichotomous facies on a Late Cretaceous rocky island as
550 related to wind and wave patterns (Baja California, Mexico). Palaios 8:385–395

551 Johnson ME, Karabinos PM, Mendia V (2010) Quaternary intertidal deposits intercalated
552 with volcanic rocks on Isla Sombrero Chino in the Galápagos Islands (Ecuador). J
553 Coast Res 26:762–768
554 Johnson ME, Ledesma-Vázquez J (1999) Biological zonation on a rocky shore boulder
555 deposit: Upper Pleistocene Bahía San Antonio (Baja California Sur, Mexico).
556 Palaios 14:569–584
557 Johnson ME, McKerrow WS (1995) The Sutton Stone: an early Jurassic rocky shore
558 deposit in South Wales. Palaeontology 38:529–541
559 Johnson ME, Silva CM da, Santos A, Baarli BG, Cachão M, Mayoral E, Rebelo AC,
560 Ledesma-Vázquez J (2011) Rhodolith transport and immobilization on a
561 volcanically active rocky shore: Middle Miocene at Cabeço das Laranjas on Ilhéu
562 de Cima (Madeira Archipelago, Portugal). Palaeogeogr Palaeoclimatol Palaeoecol
563 300:113–127
564 Johnson ME, Skinner DF, Macleod KG (1988) Ecological zonation during the carbonate
565 transgression of a Late Ordovician rocky shore (Northeastern Manitoba, Hudson
566 Bay, Canada). Palaeogeogr Palaeoclimatol Palaeoecol 65:93–114
567 Kelly SRA, Bromley RG (1984) Ichnological nomenclature of clavate borings.
568 Palaeontology 27:793–807
569 Kramberger-Gorjanović D (1889) Berichtigung bezüglich Ceratoconcha costata aus dem

Miozän von Podsused. Verh Kais-königl Geol Reichsanst 6:142

Lescinsky HL, Ledesma-Vázquez J, Johnson ME (1991) Dynamics of Late Cretaceous rocky shores (Rosario Formation) from Baja California, Mexico. Palaios 6:126−141

Lund M, Davies PJ, Braga JC (2000) Coralline algal nodules off Fraser Island, eastern Australlia. Facies 42:25−34

Mankiewicz C (1995) Response of reef growth to sea-level changes (Late Miocene, Fortuna Basin, Southeastern Spain). Palaios 10:322−336

Marrack E (1999) The relationship between water motion and living rhodolith beds in the southwestern Gulf of California, Mexico. Palaios 14:159–171

Mayer K (1864) Systematisches Verzechniss der fossilen Reste von Madeira, Porto Santo und Santa Maria nebst Beschreibung der neuen Arten. Author's edition, Zürich, p107

Meco J, Scaillet S, Guillou H, Lomoschitz A, Carracedo C, Ballester J, Betancort JF, Cilleros A (2007) Evidence for long-term uplift on the Canary Islands from emergent Mio-Pliocene littoral deposits. Global and Planet Change 57:222−234

Milne-Edwards H, Haime J (1850) A monograph of the British fossil corals. Part 1: Introduction: Corals of the Tertiary and Cretaceous formations. Monogr Palaeontogr Soc, 1−171

Multer HG (2006) A site of both sudden and slow death coral framework, together with survival attempts by corals. Coral Reefs 25:567

Okada H, Bukry D (1980) Supplementary modification and introduction of code numbers

593 to the low-latitude coccolith biostratigraphic zonation. Mar Micropaleont
5:321–325
594 Pandolfi JM, Tudhope AW, Burr G, Chappell J, Edinger E, Frey M, Steneck R, Sharma
595 C, Yeates A, Jennoins M, Lescinsky H, Newton A (2006) Mass mortality

596 following disturbance in Holocene coral reefs from Papua New Guinea. Geology
597 34:949–952
598 Perrin C, Bosence D, Rosen B (1995) Quantitative approaches to palaeozonations and
599 palaeobathymetry of corals and coralline algae in Cenozoic reefs. In: Bosence
600 DWJ, Allison PA (eds) Marine palaeoenvironmental analysis from fossils. Geol
601 Soc Lond Spec Publ 83:181–229
602 Rasser M, Piller WE (1997) Depth distribution of calcareous encrusting associations in
603 the northern Red Sea (Safaga, Egypt) and their geological implications. In:
604 Lessios HA, Macintyre IG (eds) Proceedings 8th International Coral Reef
605 Symposium, Smithsonian Tropical Research Institute, Panama 1:743-748
606 Reuter M, Piller WE (2011) Volcaniclastic events in coral reef and seagrass
607 environments: evidence for disturbance and recovery (Middle Miocene, Styrian
608 Basin, Austria). Coral Reefs 30:889–899
609 Santos A, Mayoral E, Silva CM da, Cachão M, Johnson ME, Baarli BG (2011) Miocene
610 intertidal zonation on a volcanically active shoreline: Porto Santo in the Madeira
611 Archipelago Portugal. Lethaia 44:26–32
612 Santos A, Mayoral E, Johnson ME, Baarli BG, Cachão M, Silva CM da, Ledesma-

Vázquez J (2012a) Extreme habitat adaptation by boring bivalves on volcanically active paleoshores from North Atlantic Macaronesia. Facies DOI 10.1007/s10347-011-0283-z

Santos A, Mayoral E, Baarli BG, Silva CM da, Cachão M, Johnson ME (2012b) Symbiotic association of a pyrgomatid barnacle and a coral from a volcanic

Middle Miocene shoreline (Porto Santo, Madeira Archipelago, Portugal). Palaeontology 55:173–182

Scoffin TP, Stoddart DR, Tudhope AW, Woodroffe C (1985) Rhodoliths and coralliths of Muri Lagoon, Rarotonga, Cook Islands. Coral Reefs 4:71–80

Sneed ED, Folk RL (1958) Pebbles in the lower Colorado River, Texas, a study in particle morphogenesis. J Geol 66:114–150

Steller DL, Foster MS (1995) Environmental factors influencing distribution and morphology of rhodoliths in Bahía Concepción, B.C.S., México. J Exp Mar Biol Ecol 194:201–212

Surlyk F, Sørensen AM (2010) An early Campanian rocky shore at Ivö Klack, southern Sweden. Cret Res 31:567–576

Taylor PD, Wilson MA (2003) Palaeoecology and evolution of marine hard substrate communities. Earth-Sci Rev 62:1–103

Wilson MA, Taylor PD (2001) Palaeoecology of hard substrate faunas from the Cretaceous Qahlah Formation of the Oman Mountains. Palaeontology 44:21-41

Figure captions

Fig. 1 Geographic location of the study site at Pedra de Água on Ilhéu de Cima (Porto Santo, Portugal). Star showing position of the study site

Fig. 2 Sample plan showing the layout of the census on the outcrop at Pedra de Água. The four transects are labeled A, B, C, and D. Blocks 1, 2, and 3 are the three square blocks chosen for illustration from the full layout. (16 grids to one block equal to 4 m^2)

Fig. 3 Cross-section along the exposed side of Pedra de Água outcrop, showing the position of cemented corals on top of basalt mounds and very coarse and unsorted sandy gravel with rhodoliths in the adjacent depressions

Fig. 4 Frequency data depicting the lateral zonation at Pedra de Água along the transects

650

A, B, C, and D. **a** Spatial distribution of corals. **b** Spatial distribution of bare basalt. **c** Spatial distribution of coarse bioclastic sand

Fig. 5 Frequency data depicting the lateral zonation at Pedra de Água along the transects A, B, C, and D. **a** Spatial distribution of *Gastrochaenolites* borings. **b** Spatial distribution of rhodoliths

Fig. 6 Ecologic zones mapped on the rocky paleoshore at Pedra de Água. Each block represents four square meters. **a** Block 1. **b** Block 2. **c** Block 3

Fig. 7 General view of the rocky paleoshore at Pedra de Água. **a** Closely packed coral colonies attached directly to the basalt. Scale bar: 20 cm. **b** Bivalve borings *Gastrochaenolites torpedo* in corals. Scale bar: 10 cm

Fig. 8 Generic affinities of rhodoliths from Pedra de Água. **a** *Lithophyllum* with sporangia (*black arrow*) and *Sporolithon* (*red arrow*) most commonly can occur. Scale bar: 200 μm. **b** Less common combination of *Lithophillum* and *Hydrolithon*. Scale bar: 200 μm

Fig. 9 a Matrix of very coarse and unsorted sandy gravel on which the rhodoliths rest. **b** Natural cross-section through a lumpy rhodolith with a rock core 3.5 cm in diameter. Scale bar: 2 cm

Fig. 10 Shape classification of rhodoliths from Pedra de Água based on the triangular plot formulated by Sneed and Folk (1958)

Fig. 11 Linear relationship between maximum diameter of rhodoliths (DR) and rock core (RC), with R^2=0.82

Fig. 12 Volcanic tuff directly overlying the coral biofacies (under the present see cliff) on the rocky paleoshore at Pedra de Água. Scale bar: 15 cm

Table captions

Table 1 Percentages based on census data collected for blocks A, B, and C from the mound and inter-mound communities at Pedra de Água. Each block represents 4 m^2

Table 2 Generalized paleoenvironmental interpretation from the basalt mound and inter-mound communities at Pedra de Água

Figure 1

Click here to download high resolution image

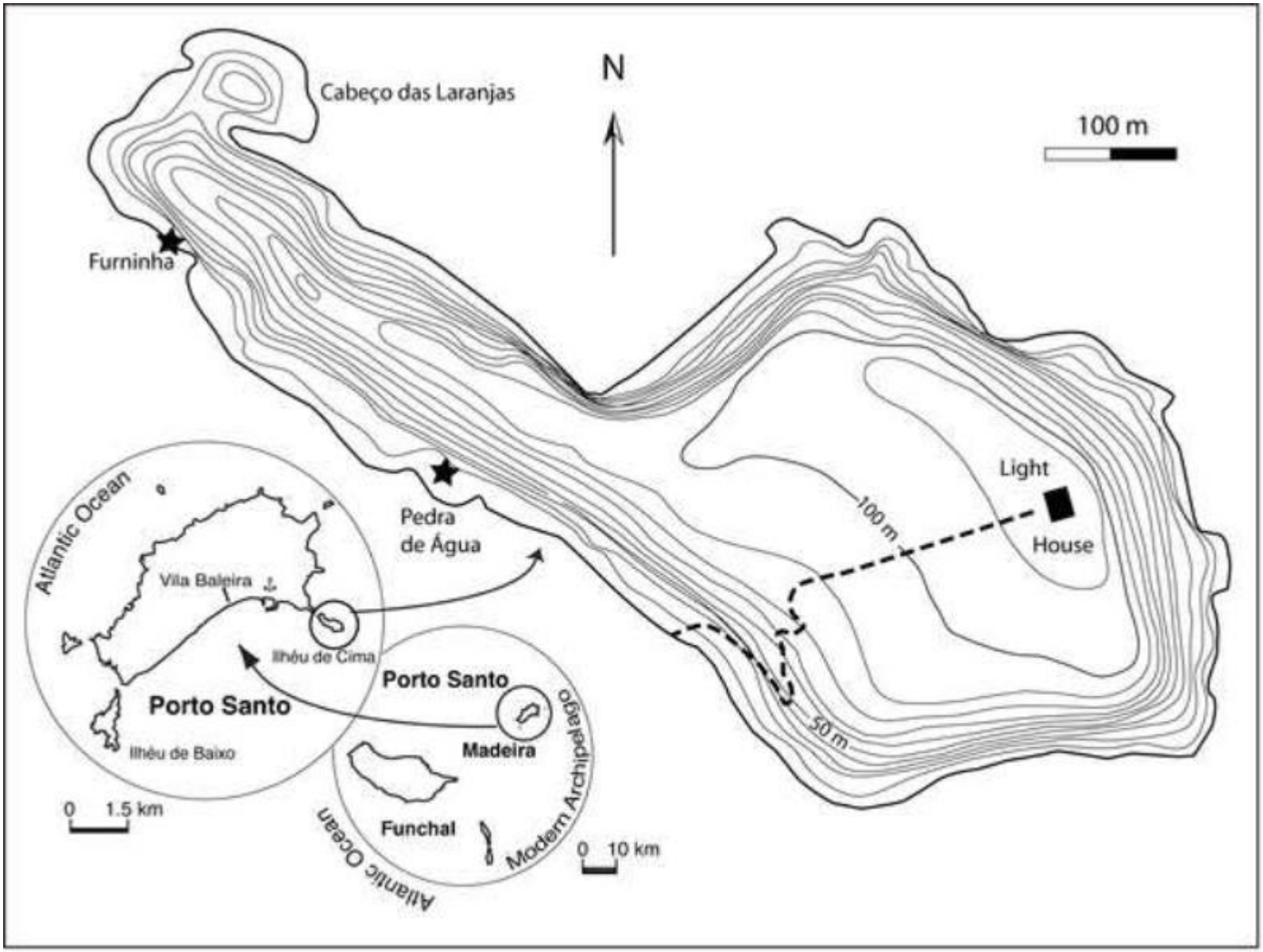

Figure 4

Click here to download high resolution image

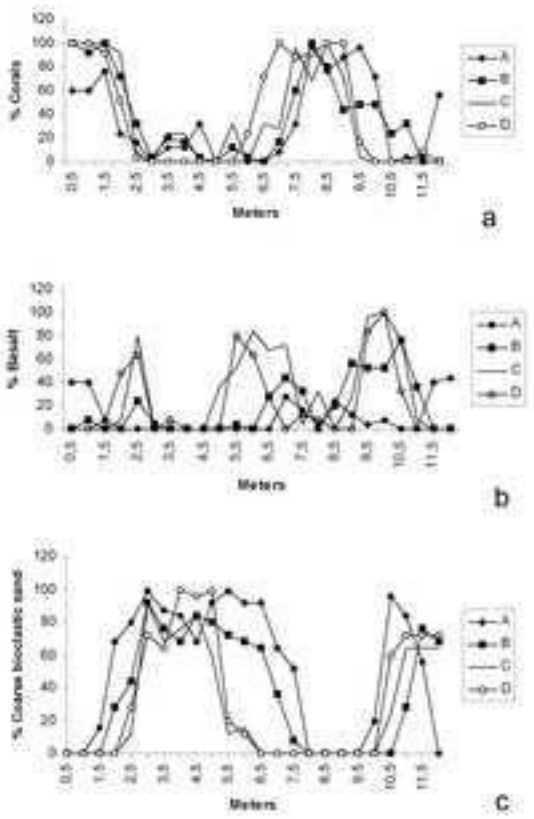

Figure 5

Click here to download high resolution image

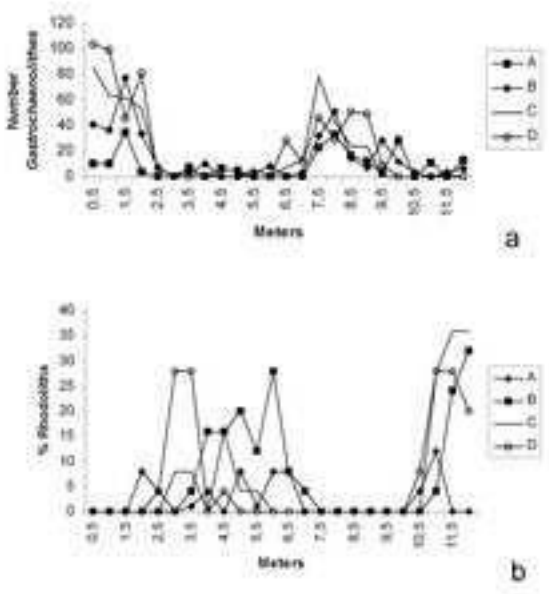

Figure 6

Click here to download high resolution image

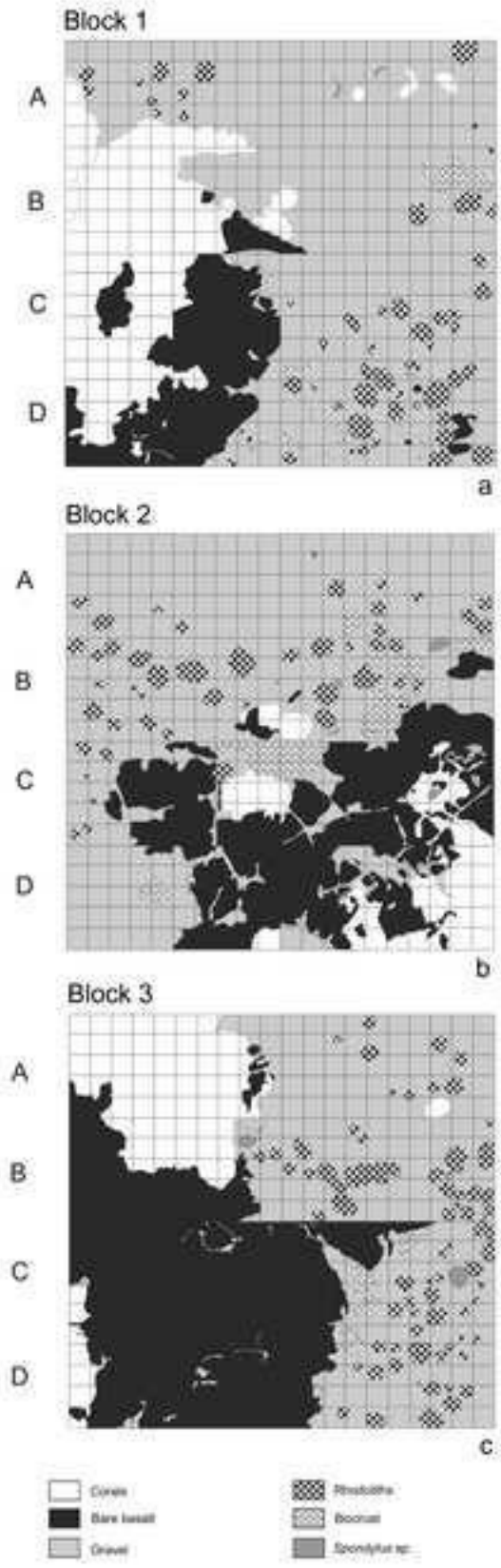

Figure 2

Click here to download high resolution image

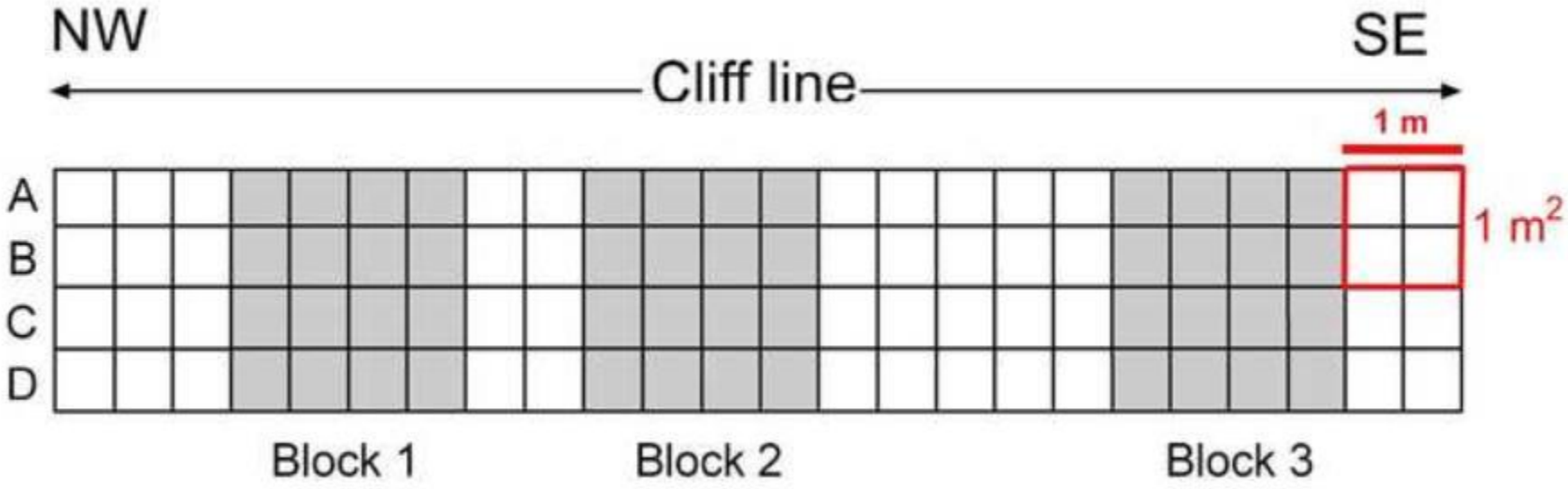

Figure 3

Click here to download high resolution image

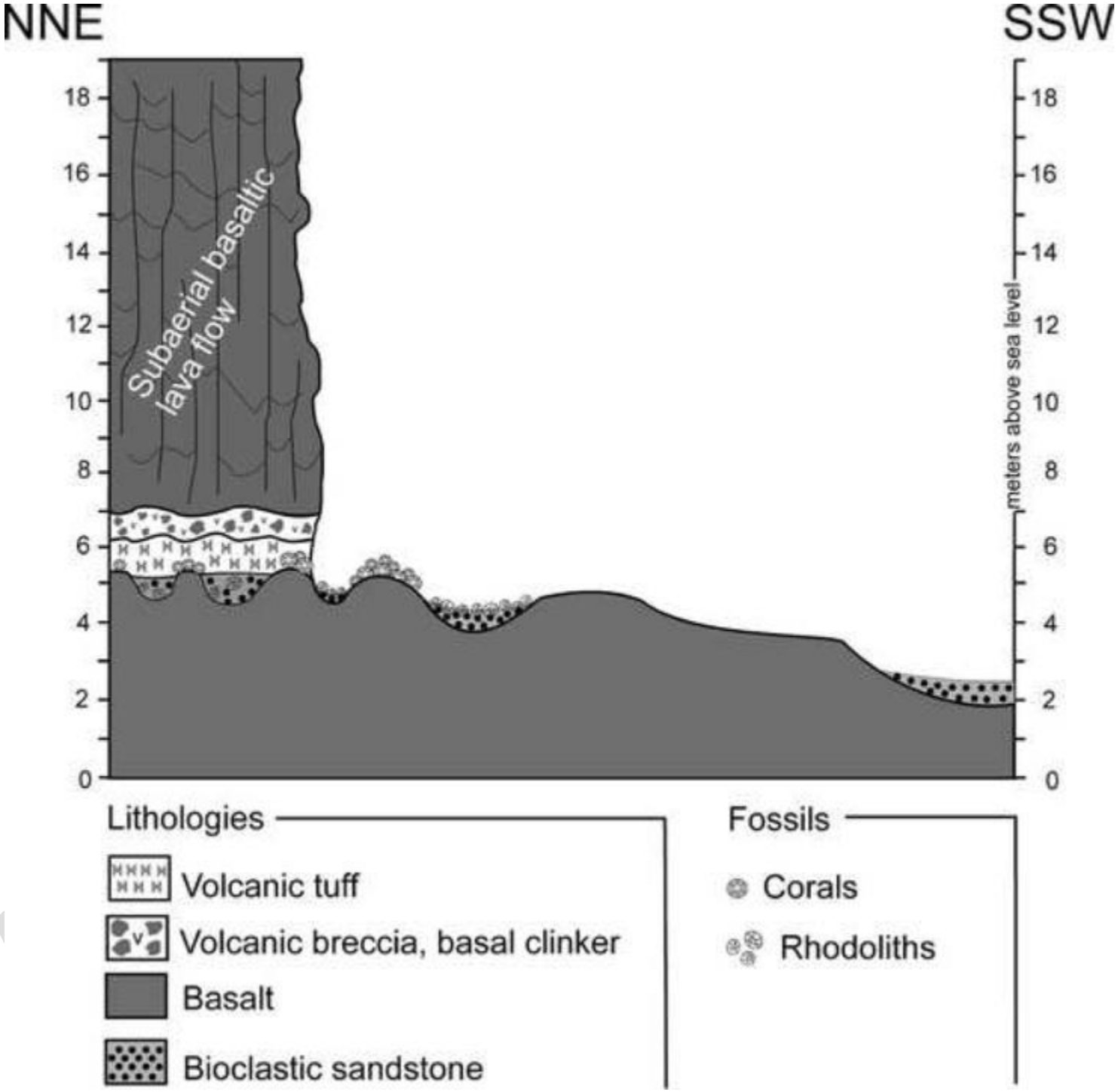

Figure 7

Click here to download high resolution image

Figure 8

Click here to download high resolution image

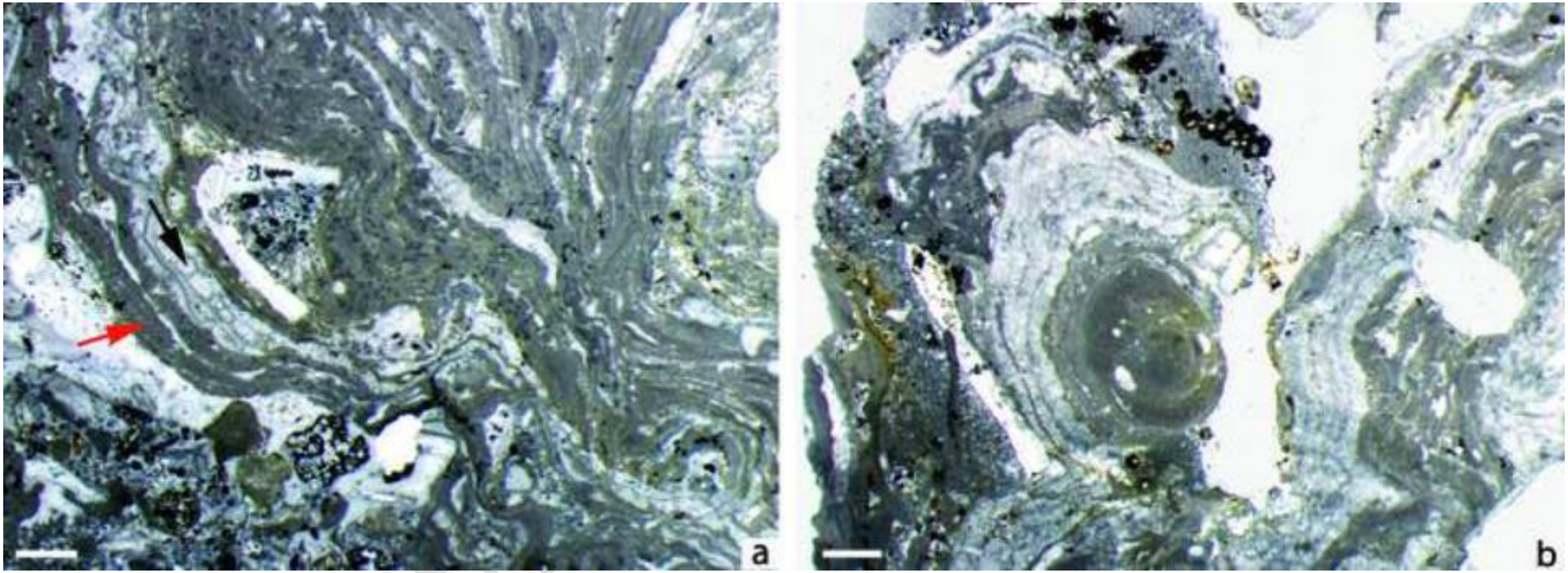

Figure 9

Click here to download high resolution image

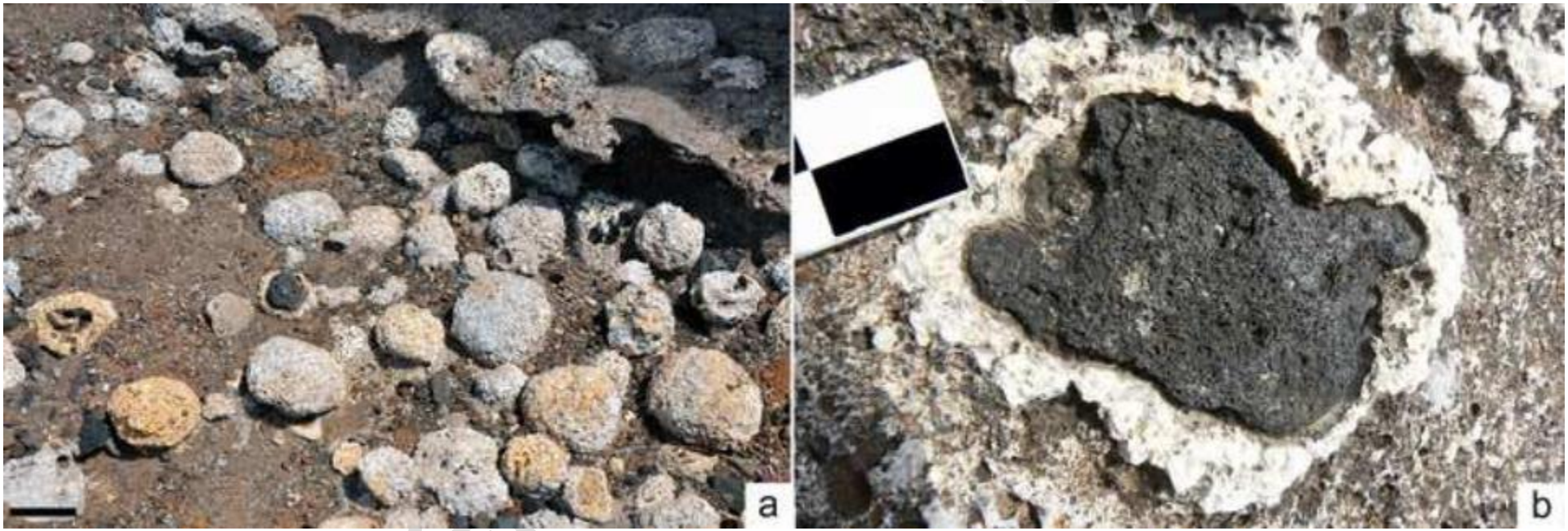

Figure 10

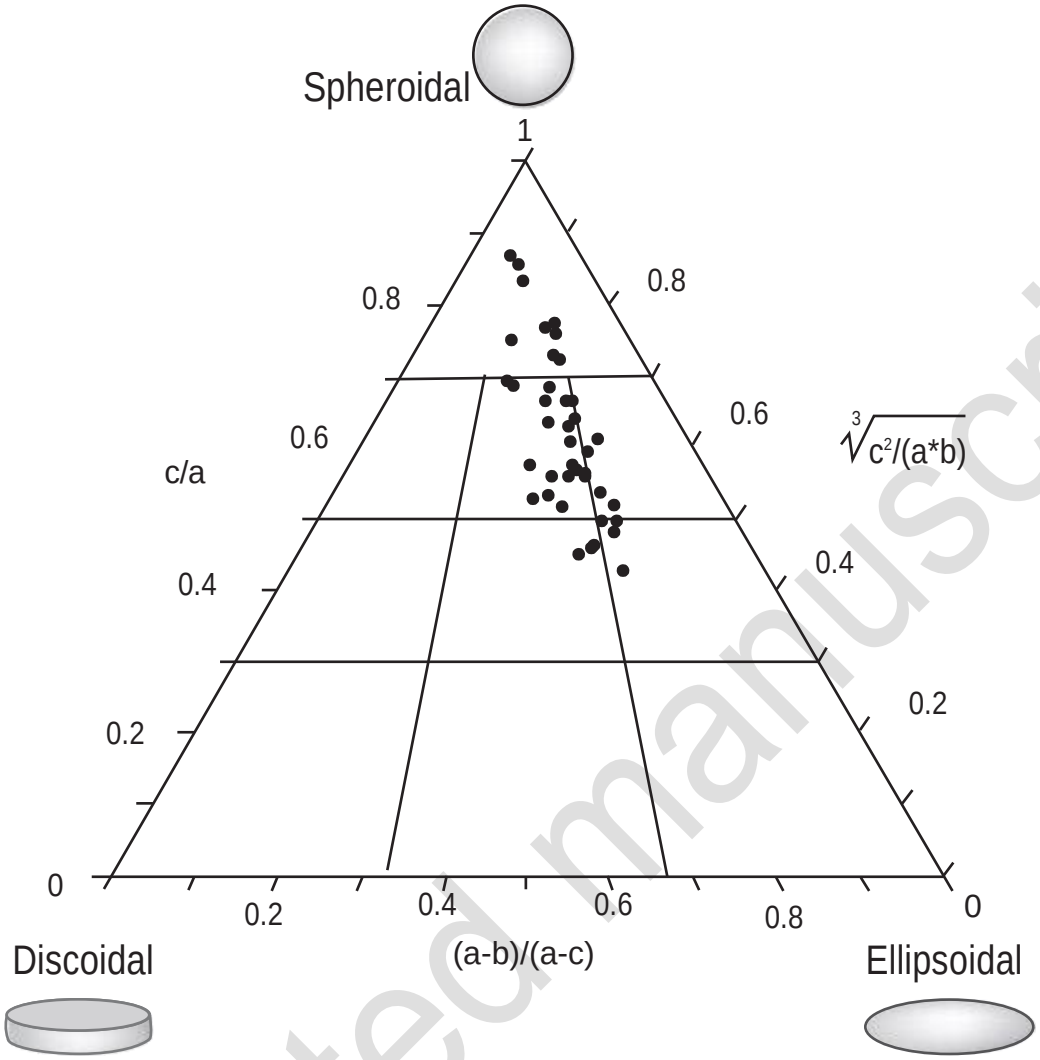

Figure 11

Click here to download high resolution image

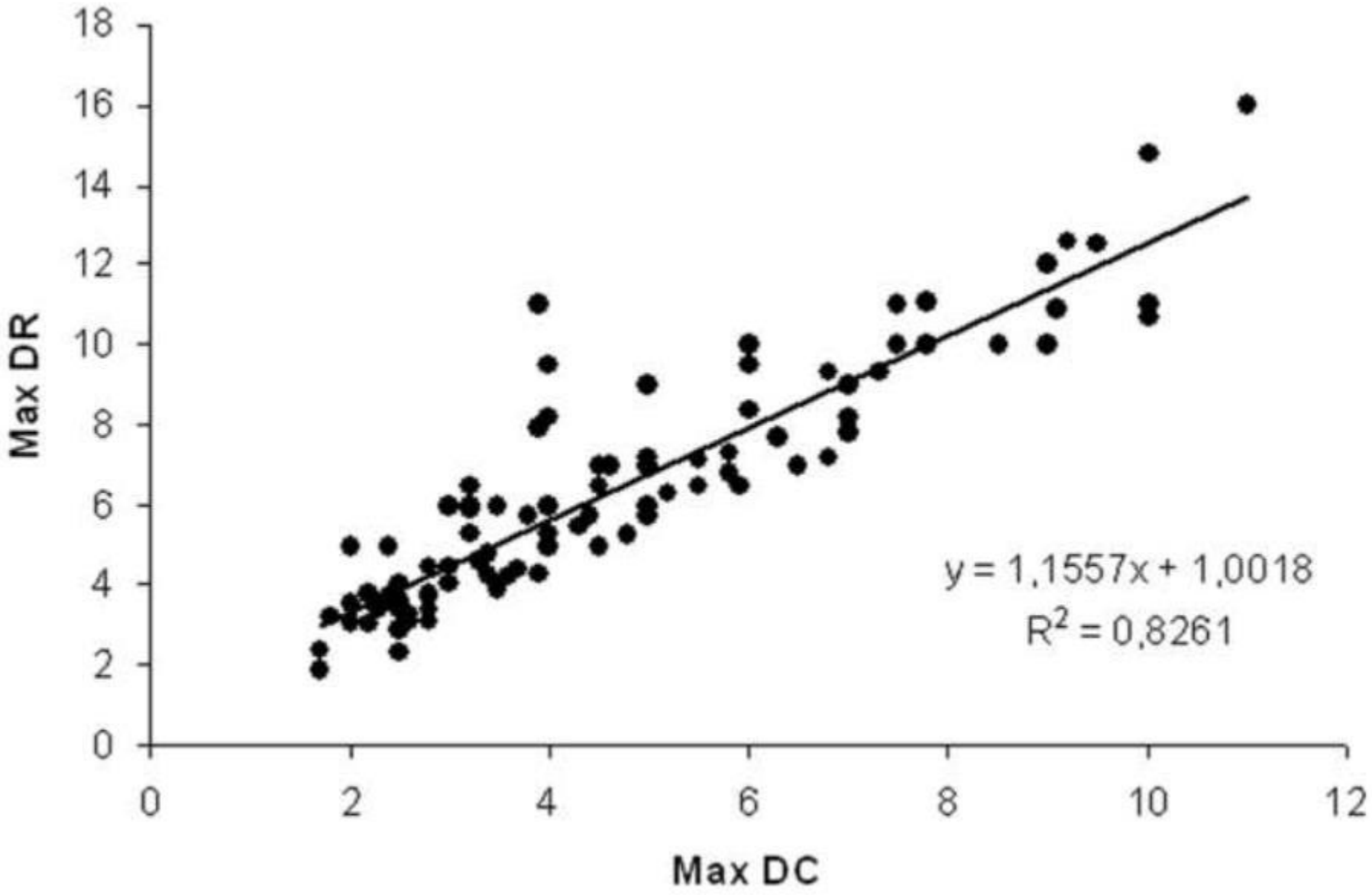

Figure 12

Click here to download high resolution image

Table 1

Table 1

Block 1	Block 2	Block 3	Average (Blocks 1 + 2 + 3)
			50
			56
			108
			3
			16
			7
			27

Table 2

	Hard substrate	Soft substrate
	Zone of coral encrustation	Zone of rhodolith pavement
Type of sediment	basalt	coarse and unsorted sandy gravel
Bioerosion	medium	low
Bioturbation	absent	absent
Rhodoliths	absent	large
Predominant algal taxa	/	polyspecific (*Lithophyllum* and *Sporolithon*)
Algal growth-forms	crusts	crusts
Paleodepth	shallow (above fair-weather wave-base)	shallow (above fair-weather wave-base)